Using the OCATA Digital Twin to Improve QoT of Optical Connections in Multiband Optical Networks

Sadegh Ghasrizadeh, Prasunika Khare, Marc Ruiz, and Luis Velasco*
Optical Communications Group - Universitat Politècnica de Catalunya. Barcelona, Spain
*email: *luis.velasco@upc.edu*

***Abstract*—Multiband optical transmission increases the complexity of network operation. In this paper, we take advantage of the OCATA time domain digital twin with the double objective of accurately estimate the Quality of Transmission (QoT) of the different channels during lightpath provisioning, as well as to improve their QoT by optimizing the detection areas of the constellation points of higher-order QAM optical signals.**

Keywords—Optical Digital Twin, Multi-band Optical Transmission

I. INTRODUCTION

Optical in-phase and quadrature (IQ) constellations enclose valuable information of the optical signal. Such information can be extracted and exploited by algorithms and models within an optical layer digital twin. In particular, the OCATA digital twin [1] models the propagation of optical signals from the transmitter (Tx) to the receiver (Rx) in the optical time domain. OCATA generates the *expected* optical signals in the time domain, which can be used to for accurate quality of transmission (QoT) estimation. The applications range from optical connection (*lightpath*) provisioning to failure management [2]. Precisely, estimation of lightpaths' QoT pre-forward error correction (FEC) Bit Error Rate (BER) was proposed in [2] based on IQ optical constellation features for C-band transmission. Thus, the probability that a symbol initially transmitted in a given constellation point is detected in the Rx out of the detection area of such constellation point was proposed as key feature for pre-FEC BER estimation.

In this paper, we tackle multiband (MB) C+L+S optical transmission, where the stimulated Raman scattering (SRS) effect creates large differences on the QoT of the different channels. In particular, we focus on lightpath provisioning, where: *i*) per channel pre-FEC BER estimation can be used to select the channel for the lightpath so as to ensure that the required QoT is met; and *ii*) optimal constellation points detection areas can be anticipated and used to program the Rx to effectively improve the QoT. Some works in the literature have proposed adapting the detection areas for nonlinear phase noise mitigation using machine learning (see e.g., [3]). Such approaches are difficult to implement in practice, as such algorithms need to run in the Digital Signal Processing (DSP). In contrast, in our approach the detection areas are computed at provisioning time, so the DSP uses them as a simple map.

II. IQ CONSTELLATION DETECTION AREAS

In OCATA, IQ optical constellation samples X are defined by a sequence of symbols $x \in X$, where every symbol belongs to one among m constellation points (CP) in an m-QAM optical signal. Then, samples are summarized as a set of semi-supervised constellation features Y, where vector Y^i defines the features characterizing the CP i. In particular, Gaussian Mixture Models (GMM) fitting is used in feature extraction (FeX) procedure to characterize a given sample X as a set of bivariate Gaussian distributions with one distribution per CP, so vector $Y^i = [\mu^I, \mu^Q, \sigma^I, \sigma^Q, \sigma^{IQ}]$ includes 5 features representing the I and Q mean position in the constellation (μ) and the real and imaginary variance and symmetric covariance terms (σ) that the symbols belonging to CP i experience around the mean.

The basic features Y can be extended with additional features. In particular, a new feature, denoted as Φout^i, was defined in [2] that computes the probability that a symbol initially transmitted in constellation point i is detected in the Rx out of the detection area of such constellation point, denoted as A^i. Φout^i is computed under the assumption that dispersion of symbols around constellation point i follow the bi-variate Gaussian distribution characterized by Y^i. For the sake of clarity, Fig. 1a reproduces from [2] an example of Φout^i for CP [-3+3i]. The contours represent the different levels of the bi-variate Gaussian distribution that characterize this CP for a given lightpath; univariate marginal distributions are provided for both I and Q axes. The area highlighted in red in both bi-variate and marginal distributions represent the region that falls out of A^i, i.e., the square delimited by vertices (-4+4i) and (-2+2i). Hence, Φout^i was formally defined as follows:

$$\Phi out^i = 1 - \phi_A(i) \tag{1}$$

$$\phi_A(i) = P\left(x \subset A^i \middle| x \sim N(Y^i)\right) \tag{2}$$

Note that the estimated pre-FEC BER can be computed based on Φout^i for all the CPs, e.g., assuming equal probability of the symbols. Then, in view of eqs. (1) and (2), Φout^i and consequently, the final QoT, can be improved by changing the shape of A^i in the Rx. To illustrate that, Fig. 1b shows an adapted detection area for CP i to minimize total Φout, i.e., not only that for CP i. However, finding the optimal A^i for every CP is a complex task, so algorithmic solutions for computing a set of near-optimal detection areas in limited times are required.

III. CPS DETECTION AREAS AND BER ESTIMATION

This section proposes a fast method to compute the near-optimal detection areas for the CPs, as well as the resulting BER. Table 1 presents the used notation. The method is based on dividing the whole coordinate IQ plane (A) into k small

978-3-903176-62-1

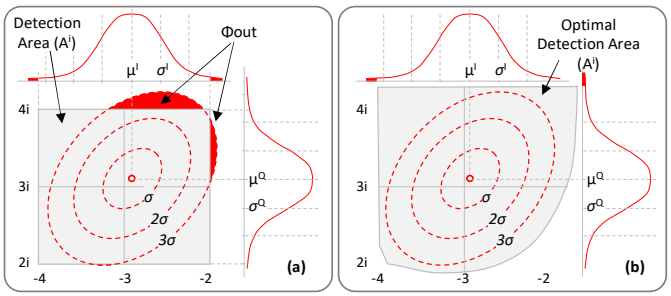

Fig. 1. Example of *Φout* feature and regular (a) (reproduced from [2]) and optimized (b) detection area for CP -3+3*i*.

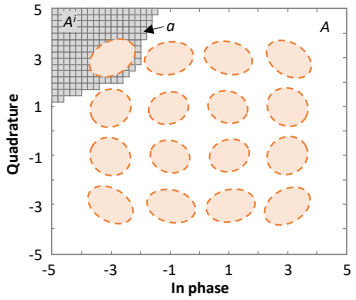

Fig. 2. Definition grid for 16-QAM signal constellations.

Table 1: General notation.

X	Set of symbols, index x.
Y^i	Features of CP i
A	The whole coordinate plane, which is divided into small squares a.
k	Number of squares areas a, each of size δxδ.
A^i	Detection area for CP i.
$\phi_A(i)$	Probability of a symbol from CP i is received inside the detection area A^i.
Φout^i	Complementary probability of ϕ_A.
$\varphi_a(i)$	Probability of a symbol from CP i is received inside the small square $a \in A^i$.

square areas a to create a grid. Fig. 2 shows an example for a 16-QAM signal, where A is defined by the corner points [5+5*i*] and [-5-5*i*]. The detection area for CP [3+3*i*] is shown as a set of small areas. Then, the probability of receiving a symbol originally transmitted in CP i can be now computed as eq. (3), and therefore, Φ_A can be alternatively computed as eq. (4).

$$\varphi_a(i) = P(x \subset a | x \sim N(Y^i)) \quad (3)$$

$$\phi_A(i) = \sum_{a \in A^i} \varphi_a(i) \quad (4)$$

With these definitions, the proposed method consists in assigning each of the small areas a to the detection area A^i of the CP i with the highest probability Algorithm 1 shows the pseudocode of the algorithm that receives features Y, the coordinate plane A divided into small areas, and the number m of CPs in the signal, and computes the vector of detection areas $[A^i]$, where each area defines a subset of small areas of the whole coordinate plane. The complexity of Algorithm 1 is $O(k \cdot m \cdot p)$, where p is the complexity of computing $\varphi_a(i)$.

Algorithm 1. Compute Detection Areas

INPUT: *Y, A, m* **OUTPUT:** $[A^i]$

```
1:  A^i ← Ø, for each i:1..m
2:  for each a in A do
3:    a.i ← 0
4:    a.maxProb ← 0
5:    for i: 1..m do
6:      if φ_a(i) > a.maxProb then
7:        a.maxProb ← φ_a(i); see eq. (3)
8:        a.i ← i
9:    A^{a.i} ← A^{a.i} ∪ a
10:  return [A^i]
```

Algorithm 2. Pre-FEC BER estimation

INPUT: *X, m* **OUTPUT:** *BER*

```
1:  Y←FeX(X)
2:  A←CreateGrid()
3:  [A^i] ← ComputeDetectionAreas(Y, A, m)
4:  Φout←0
5:  for i=1..m do
6:      φ_A(i) ← 0
7:      for each a in A^i do
8:          φ_A(i) ← φ_A(i) + a.maxProb
9:      Φout^i ←1- φ_A(i)
10:     Φout←Φout+ Φout^i / m
11: return Φout / log2 m
```

Once the detection areas are computed, the pre-FEC BER can be estimated based on probabilities Φout^i computed on the corresponding detection area A^i for each CP. Algorithm 2 presents the pseudocode that receives as input a constellation sample X and the number m of CPs in the signal, and returns the estimated BER. The algorithm first computes the features Y using GMM fitting [1] (line 1 in Algorithm 2). A grid is next created by dividing the coordinate plane into small non-overlapping squares (a) with width and height equal to δ and the detection areas are obtained by using Algorithm 1 (lines 2-3). Next, Φout is estimated by computing Φout^i for each CP i on the defined grid and averaging for the number of CPs (lines 4-10). Finally, the BER is estimated and returned (line 11).

IV. Results and Conclusions

For evaluation, we considered a multiband C+L+S scenario with full spectrum usage, leading to 337 channels with 50 GHz channel spacing. Ranges of channels for the S, C and L bands are [1-128], [129-215], [216-337]. The MATLAB-based simulator of a coherent WDM system developed in [4] was used to generate IQ constellations for 16QAM@32GBd signals shaped by a root-raised cosine filter with a 0.06 roll-off-factor.

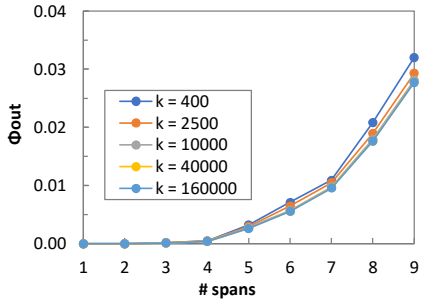

Fig. 3 Estimated pre-FEC BER for different number of areas *k*.

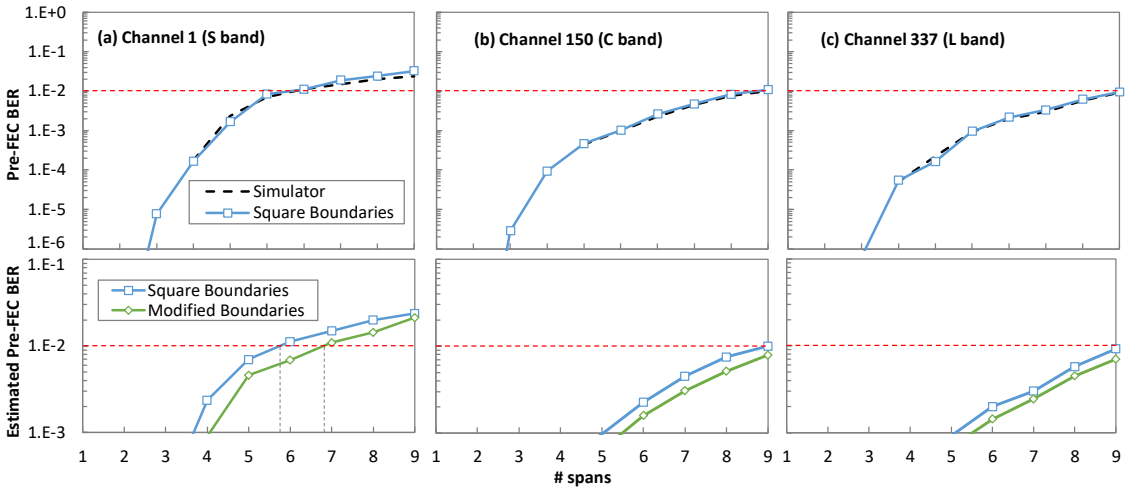

Fig. 4 Real and estimated pre-FEC BER with squared and optimized detection areas vs # spans for channel 1 (a), 150 (b), and 337 (c).

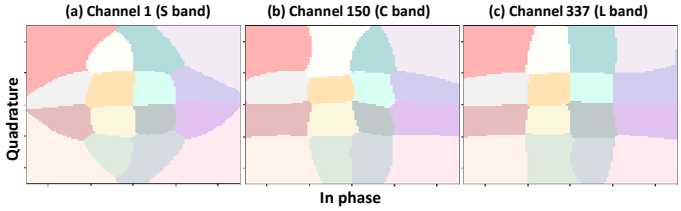

Fig. 5 Example of optimal detection areas (k=10,000) for 5 spans.

Pseudorandom binary sequences of length 2^{14} are used as input of every channel. The signal is propagated through standard single mode fiber, with a launch power of 0 dBm and collected at the Rx side after a number of 80-km fiber spans. Spans are modeled by solving the nonlinear Schrödinger equation, whereas ideal inline OAs are modelled as erbium-doped fiber amplifier (EDFA) for the C and L bands and thulium-doped fiber amplifier (TDFA) for the S band. An adaptive step size algorithm is included to further reduce the computation time required. Finally, at the Rx, a DSP block performs ideal chromatic dispersion compensation and phase recovery.

Let us first analyze the number of areas k that need to be considered in Algorithm 2 to obtain accurate Φout computations. Fig. 3 illustrates the convergence of Φout with k for channel 337; similar results can be obtained for other channels. We observe that very small error is obtained when more than 10,000 areas are considered, which greatly limits the complexity of Algorithm 1 to compute the detection areas.

Fixing k=10,000, Fig. 4 shows the evolution of the pre-FEC BER of three channels, each one from a different band, as a function of the number of fiber spans. The upper row of graphs compares the pre-FEC BER measured by the simulator and the one estimated using Algorithm 2, assuming square boundaries for the detection areas. We observe that the estimation of the pre-FEC for the three channels using Φout is very accurate, in line with the results in [2] for the C band. The graphs at the bottom in Fig. 4 shows the estimated pre-FEC BER when the detection areas are optimized using Algorithm 1. We observe and improvement of the resulting pre-FEC BER in all three channels and independently of the number of spans that the signal crosses. Let us assume a pre-FEC BER threshold equal to 1e-2. Interestingly, we observe that the maximum number of spans supported by the signal, heavily depends on the selected channel. Then, a clear application of the OCATA digital twin is during the provisioning phase to select the channel for the lightpath so as to ensure that the pre-FEC BER threshold is not exceeded. In addition, by configuring the optimal detection areas in the Rx, the maximum distance that can be setup for a lightpath using each channel can be effectively extended. We observe in the graphs at the bottom in Fig. 4 that 1 additional span can be clearly added in the case of using channel 1 without exceeding the pre-FEC BER threshold when the optimized detection areas are used, w.r.t. the regular ones; a similar observation can be obtained from the channel 150 and 337. For illustrative purposes, Fig. 5 shows the optimized detection areas for a lightpath with 6 spans using channels 1, 150 and 337. We observe the different shapes of the detection areas for the different channels.

In conclusion, we have shown an accurate and low complex method for estimating the pre-FEC BER for any channel in the C+L+S bands, which has a clear application during lightpath provisioning, as it helps to select the right channel. In addition, programming the Rx with the optimal detection areas for the selected lightpath can improve the pre-FEC BER of the lightpath and extend its total distance. Note that such distance extension can highly reduce the blocking probability for lightpath provisioning due to distance limitations.

ACKNOWLEDGEMENT

The research leading to these results has received funding from the European Community through the MSCA MENTOR (G.A. 956713) and the HORIZON SNS JU SEASON (G.A. 101096120) projects, the AEI through the IBON (PID2020-114135RB-I00) project, and the ICREA institution.

[1] D. Sequeira *et al.*, "OCATA: A Deep Learning-based Digital Twin for the Optical Time Domain," J. Opt. Commun. Netw., vol. 15, pp. 87-97, 2023.

[2] M. Devigili *et al.*, "Applications of the OCATA Time Domain Digital Twin: from QoT Estimation to Failure Management," J. Opt. Commun. Netw., vol. 16, 2024.

[3] M. Li *et al.*, "Nonparameter Nonlinear Phase Noise Mitigation by Using M-ary SVM for Coherent Optical Systems," IEEE Photon. J., vol. 5, 2013.

[4] P. Khare *et al.*, "SSMS: A Split Step MB Simulation Software," in proc. ICTON, 2023.